Fire Safety Journal 91 (2017) 845–854

Contents lists available at ScienceDirect

Fire Safety Journal

journal homepage: www.elsevier.com/locate/firesaf

IAFSS 12th Symposium 2017

Utilization of remote sensing techniques for the quantification of fire behavior in two pine stands

Eric V. Mueller[a], Nicholas Skowronski[b], Kenneth Clark[c], Michael Gallagher[c], Robert Kremens[d], Jan C. Thomas[a], Mohamad El Houssami[a], Alexander Filkov[e,f], Rory M. Hadden[a,*], William Mell[g], Albert Simeoni[h]

[a] BRE Centre for Fire Safety Engineering, University of Edinburgh, Edinburgh, UK
[b] Northern Research Station, USDA Forest Service, Morgantown, WV, USA
[c] Northern Research Station, USDA Forest Service, New Lisbon, NJ, USA
[d] Center for Imaging Science, Rochester Institute of Technology, Rochester, NY, USA
[e] School of Ecosystem and Forest Sciences, University of Melbourne, Creswick, Australia
[f] Department of Physical and Computational Mechanics, Tomsk State University, Tomsk, Russia
[g] Pacific Wildland Fire Sciences Laboratory, USDA Forest Service, Seattle, WA, USA
[h] Jensen Hughes, Inc., Framingham, MA, USA

ARTICLE INFO

Keywords:
Wildfires
Flame spread
Remote sensing
Fuel structure
Wind

ABSTRACT

Quantification of field-scale fire behavior is necessary to improve the current scientific understanding of wildland fires and to develop and test relevant, physics-based models. In particular, detailed descriptions of individual fires are required, for which the available literature is limited. In this work, two such field-scale experiments, carried out in pine stands under mild conditions, are presented. A particular focus was placed on non-intrusive measurement, as the capabilities of advanced remote sensing techniques, along with more traditional approaches, are explored. A description of the fires is presented, with spread occurring predominantly in the surface fuels with intensities in the range of 200–4400 kW m^{-1}, and punctuated by isolated regions of crown fire. The occurrence of crown fire is investigated and linked to regions of greater canopy density, and it is found that the total fire intensity may increase locally to as much as 21,000 kW m^{-1}. The light winds do not appear to play a direct role in the changes in fire behavior, while fuel structure may be important. The measurements described herein provided a reasonable overall description of the fires, however, the current resolution (both spatial and temporal) falls short of definitively explaining some transitional aspects of the fire behavior, and future improvements are suggested.

1. Introduction

Significant gaps remain in the current understanding of the contribution of different driving mechanisms to the spread of large-scale outdoor fires, such as wildland fires [1]. A particular difficulty lies in the fact that laboratory tests, while offering many insights, cannot fully account for and scale the relevant conditions and phenomena [2]. Thus, field-scale measurements of fire behavior are paramount for increasing the current scientific understanding and developing models of fire behavior, particularly those employing detailed physics-based formulations [3].

Experimental measurement of fire behavior has been conducted in the field for grasslands (e.g. [4–7]), shrublands (e.g. [8–10]), and forested environments (e.g. [11–13]). However, the collection of work is limited by the fact that large scale experimental fires can be dangerous and resource intensive, with a significant potential for shortcomings. High intensity fires can also prove to be difficult to instrument successfully. Further, many studies report only statistics for a series of fires, without examining any particular fire in detail (e.g. [12]). This is valuable for creating empirical models, but does not provide sufficient information required for detailed analysis of singular fires (which often have dynamic behavior in the field), such as comprehensive time histories [4–6,9]. With appropriate measurement, a single spreading fire can offer insight into detailed aspects of fire behavior at different locations in space and time [9]. This kind of analysis is required for exploring the physics and testing detailed models against specific experiments.

In this study, two experimental fires were carried out in the context of several larger objectives, including quantifying the effect of fire (particularly prescribed fire) on fuel loading and structure, and

* Corresponding author.

http://dx.doi.org/10.1016/j.firesaf.2017.03.076
Received 15 February 2017; Accepted 15 March 2017
Available online 10 May 2017
0379-7112/ © 2017 Elsevier Ltd. All rights reserved.

Nomenclature

c_p	specific heat (kJ kg^{-1} K^{-1})
I	fireline intensity (kW m^{-2})
m	fuel load (kg m^{-2})
R	rate of spread (m s^{-1})
T	temperature (K)
u	wind speed (m s^{-1})

Greek

Δh_c	heat of combustion (kJ kg^{-1})
Δm	fuel consumption (kg m^{-2})
ρ	gas density (kg m^{-3})

subscripts

$_i$	initial (pre-fire)
$_o$	ambient

providing datasets necessary to test detailed physics-based fire behavior models. However, the current study aims to develop a broad assessment of fire behavior, while examining the capabilities of non-intrusive measurements to fully explain the observations. Detailed measurements of the flame region are ultimately important, particularly for model testing, and were a part of the overall study. Nevertheless, it is worth critiquing how well more general measurements (i.e. characteristics of wind and fuel) can explain the fire behavior. These types of measurements, along with spread rate and some flame geometry, are the most often made in field-scale experiments, as wind and fuel are known to drive fire behavior. However, it must be examined whether these efforts are sufficient to increase the current understanding of the underlying mechanisms. This work also provides the baseline inputs necessary for the subsequent modeling of fire behavior in this type of environment [14].

Here, we take advantage of the relatively recent development and improvement of advanced remote sensing techniques, which allow for detailed measurement of both fuel structure and local fire behavior for individual fires. Aerial infrared (IR) and Light Detection and Ranging (LiDAR) sensors were utilized to monitor the fire spread and canopy fuel structure, respectively. Fuel measurements were supplemented by destructive sampling, and ambient wind conditions were recorded outside the burn areas. An assessment of the respective influences of fuel and wind conditions on changes in fire behavior was carried out to understand their relative importance.

2. Methods

2.1. Study site

The two experiments (EX1 and EX2) were carried out in the Pinelands National Reserve (PNR) of New Jersey, United States. This reserve covers an area of approximately 445,000 ha, and is the site of an active prescribed fires program by the New Jersey Forest Fire Service (NJFFS) and federal wildland fire managers. This is intended to reduce fuel loads and thus mitigate fire risk [15]. The climate is classified as cool temperate, with mean monthly temperatures of 0.3 °C in January and 24.3 °C in July, and mean annual precipitation is 1159 mm. The basic geography is a relatively flat coastal plain with low-angle slopes and a maximum elevation of 63.5 m, with primarily well-drained sandy soil [16]. Upland forests of pine and oak dominate this landscape, which have an extensive history of prescribed fire treatments and wildfire, and wetlands and short statured pine plains also occur [17,18].

The forest type was pitch-pine scrub-oak, dominated in the canopy by pitch pine (*Pinus rigida* Mill.), with intermittent clusters of post-oak *(Quercus stellata* Wangenh.) and white oak *(Quercus alba* L.) in the sub-canopy. The understory contained a shrub layer of huckleberry (*Gaylussacia* spp.), blueberry (*Vaccinium* spp.), and scrub oaks (*Quercus* spp.) (Fig. 1a). Pre-existing access roads were used as the block perimeters, and both blocks were split by an unmaintained fuel break - oriented north to south (Fig. 1b,c).

The experiments were carried out in early March, before the growth of new vegetation in the spring. The window between snow melt and deciduous leaf expansion corresponds to the time which prescribed fires are conducted by the NJFFS in the PNR, putting this study directly the context of conditions typically observed during prescriptive management operations. Additionally, a large majority of major wildfires in the PNR occur prior to leaf expansion. Therefore, an understanding of fire behavior during this time is relevant to fuel management and wildfire suppression activities.

Both fires were initiated with the wind linearly along the length of the north road (~330 m and ~207 m long, respectively), using a gasoline drip torch. Flame fronts progressed as head fires in a south

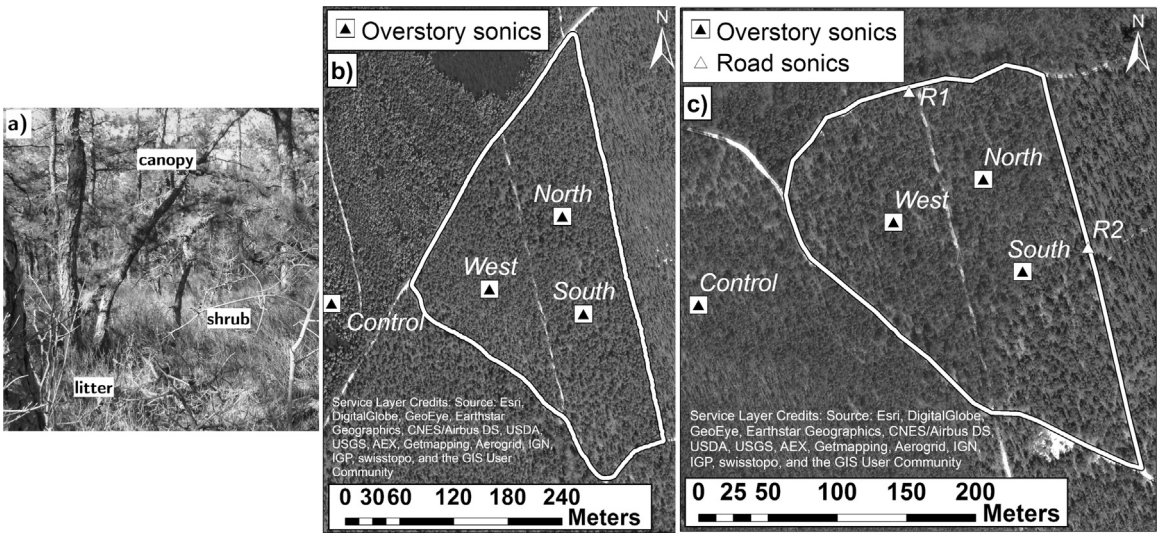

Fig. 1. (a) Typical pre-burn vegetation conditions, representative of both experiments, and layout of the (b) EX1 and (c) EX2 burn blocks, with anemometer locations noted.

easterly direction. Both blocks included a 3 m wide fuel break down the center of each unit (Fig. 1). In EX1, a secondary fireline was subsequently lit along the southwest road as a safety precaution, however the analysis here focuses on the initial region of head fire in the northern half of the block, judged to be unaffected by this second ignition.

2.2. Fire measurements

The fire environment for each experiment was monitored using three 12.5 m overstory towers, while a fourth identical tower monitored ambient conditions ~100 m to the northwest of the burn units in nearly identical forest structure conditions (Fig. 1). Tower locations within the block were selected so as to reduce any directional bias and clustering of measurements, allowing for flexible choice of an ignition line, given the conditions leading up to the burn. At the top of each, a sonic anemometer measured air temperature and wind velocity in three components (RM 80001 V, R. M. Young Co.). These data were logged at a rate of 10 Hz by dataloggers (CR3000, Campbell Scientific). The choice of 12.5 m corresponded to roughly maximum canopy height, consistent with previous long-term flux studies carried out in the PNR [19]. Two additional sonic anemometers were placed at 3 m on the north and east roads for EX2 (Fig. 1) to monitor potential wind channeling, and sampling was carried out at 1 Hz by dataloggers (CR-1000, Campbell Scientific). Infrequent gaps in the sonic anemometer data were filled via linear interpolation.

A time history of the fire progression was recorded from an aircraft using Rochester Institute of Technology's Wildfire Airborne Sensor Program (WASP) [20]. The WASP provided time-stamped, othomosaiced, and georeferenced long-wave infrared (8.0–9.2 μm) and visible (0.4–0.9 μm) spectral band images, at a resolution of 640×512. Still images were obtained for each flyover of the aircraft. This did not allow for a fixed frequency of images; however, time stamps for each image are reported as necessary.

2.3. Fuel measurements

Surface fuel loading assessments were conducted pre-and post-burn via destructive sampling at 12 plots spaced relatively evenly across each burn unit. Pre-burn sampling was conducted within 6 weeks prior to the burn, and post-burn sampling was conducted within 1–2 weeks after burning. At each plot, three destructive sampling clip plot areas of 1 m^2 were selected where surface fuels were collected and field sorted as forest floor and shrub material. These samples were further sorted into fine fuels (leaf litter), reproductive material (pine cones, acorns, and catkins), and live and dead woody material (live shrub stems, dead shrub stems, downed twigs and small branches) [21]. Live and dead woody material was further differentiated into three moisture time-lag diameter classes (1-hr: 0–6.35 mm, 10-hr: 6.35–25.4 mm, 100-hr: 25.4–76.2 mm). In this study, only small diameter fuels (needles and wood with diameter < 6.35 mm) are considered. This follows the assumption that a significant percentage of small diameter fuel is consumed in the flaming region [22]. Post-burn samples in each plot were collected at three new locations, relative to pre-burn sample locations, at each of the 12 plots. Fuel loading and consumption data presented represents dry masses of sorted material following processing at 70 °C in convection ovens for a minimum of 48 h. Fuels data for four plots of EX1 have been omitted, as they were impacted by the secondary, unintended ignition described in Section 2.1, reflecting behavior and consumption conditions beyond the scope of this study.

Fuel moisture content (FMC was estimated from samples of pitch pine needles, shrub stems, and woody fuels on the forest floor taken at an adjacent location during each burn. Samples were placed in sealed plastic bags and stored in coolers, and then weighed before and after drying at 70 °C to estimate fuel moisture content.

Airborne Light Detection and Ranging (LiDAR) was used to provide remote measurement of canopy fuel structure and density. Three flights of data (covering an area that includes both blocks) are used: one before EX1, one following EX1 in the same year, and one following EX2. Using these, canopy bulk density (CBD) was modeled, at a resolution of 10 m×10 m×1 m, from the surface up to canopy height. Details of the calibration technique can be found in Clark et al. [23] and Skowronski et al. [24]. As with the surface fuels, CBD estimates only include small diameter fuels (needles and wood of diameter < 6.35 mm). By integrating the CBD estimates along vertical profiles and comparing pre- and post-fire values, maps of loading and consumption were generated. This integration did not include the bins in the first 1 m above the ground, as this represented a potential overlap with the shrub data, which has been accounted for by destructive sampling. It should be noted that an error was identified in certain regions of the LiDAR data covering EX1. This has been traced back to a systematic error in the ALS data that is related to multiple-time-around (MTR) zones. These MTR zones occur where multiple light pulse reflections impact the LiDAR detector at the same time, leading to a spatially systematic loss of data. Despite this, the data can be used to clearly identify regions of consumption in the portion of the EX1 block where this study is focused. This issue was similarly avoided in EX2, as the site was located between MTR zones and only the edges were marginally impacted. Loading was obtained by integrating pre-fire data over height, while consumption was obtained by subtracting pre- from post-fire values before integrating.

2.4. Fire spread and energy calculation

Spread rates were obtained from fire isochrones created using the aerial IR imagery. The isochrones were drawn by mapping the gradient of pixel intensity for each image and manually tracing a curve along the highest gradient in *ArcGIS 10.1* (ESRI, Redlands, CA), and were checked for consistency against visible spectrum imagery. Spread rate was estimated by measuring the distances between fire isochrones. These measurements were made at roughly 10 m intervals along the iscochrones (excluding locations where the center line or edges had a clear influence) in order to obtain a mean forward spread and an estimate of variability. Due to the fact that each isochrone is typically comprised of multiple orthomosaiced images, time stamps are considered accurate ± 3 s.

In order to characterize observed fire behavior, it is useful to estimate a fireline intensity I, which indicates the energy release rate per unit length of fire front [25]:

$$I = \Delta h_c \cdot \Delta m \cdot R. \quad (1)$$

Here, Δh_c is taken as 18700 kJ kg^{-1} [26]. This is the low heat of combustion and is an estimate based on an average value for a number of different fuel species and types (e.g. wood, needles, bark). This is not specific to species in the PNR, however, studies have shown that the typical variation is only on the order of ± 10% [25,27]. Corrections can be made to account for completeness of combustion and mass consumption during smoldering combustion, but for the purposes of a general assessment of fire behavior, this value is sufficient.

3. Results

3.1. Experimental conditions and fire spread

A summary of the experimental conditions is given in Table 1 and FMC is given in Table 2. Data for the forest floor FMC was not available for EX2, however, both fires were carried out under light winds and cool temperatures with moderate FMC, representative of the spring prescribed burn season [21]. Given the seasonal similarity of ambient weather conditions that drive dead fuel moisture dynamics and the consistency of the other values between years, the forest floor FMC is

Table 1
Summary of the general burn conditions.

Variable	EX1	EX2
Area (ha)	6.71	4.25
Date	March 5th, 2013	March 11th, 2014
Ignition time (EST)	11:53	12:46
Mean ambient temperature (°C)	7.7 (0.2)	18.4 (0.4)
Mean horizontal wind at 12.5 m (m s^{-1})	1.8 (0.9)	3.9 (1.8)
Mean horizontal wind at 12.5 m (°)	314 (43)	300 (29)
Mean relative humidity (%)	39.4 (0.6)	31.4 (1.4)

Table 2
Mean (standard deviation) fuel moisture content (FMC) measurements.

Location	Fuel type	EX1 FMC (%)	EX2 FMC (%)
Canopy (pitch pine)	Live needles	114.4 (2.5) *(n=7)*	117.7 (9.3) *(n=12)*
	Live stems, 0–6.35 mm	85.2 (6.7) *(n=7)*	92.2 (10.8) *(n=12)*
Understory	Shrub stems, 0–6.35 mm	60.9 (7.3) *(n=8)*	56.8 (11.9) *(n=8)*
	Oak stems, 0–6.35 mm	61.2 (5.3) *(n=5)*	53.6 (15.4) *(n=12)*
Forest floor	Wood, 0–6.35 mm	15.3 (2.4) *(n=7)*	15[a]
	Needle litter	22.5 (11.2) *(n=8)*	30[a]

[a] Direct measurement not available, estimated with historical data and expert judgement.

expected to be comparable to EX1. Estimates are given based on other measurements and informed by historical data and experience.

The total duration of fire spread in EX1 was around 60 min, though approximately 82% of the unit was burned within the first 25 min (due in part to the spread from the secondary ignition line) (Fig. 2). Spread after P7 is not considered in this analysis, due to the complicating interaction of the secondary fire front. Fire spread in EX2 was also rapid initially, with approximately 44% of the unit experiencing fire in the first 15 min (Fig. 2), however, the full burn lasted closer to 80 min. The main direction of fire spread for both experiments was initially perpendicular to the orientation of the ignition line. In both cases, sharp inconsistencies can be seen in the fire isochrones towards the center of the burn block. These are a result of the center control lines, which had very low fuel loads. However, spotting and direct flame contact with fuels on the opposite side resulted in fire spread across the break.

The fires were observed to spread primarily as surface fires, with limited localized torching of tree crowns. Visual observation confirmed that this was often induced by vertical flame spread up individual tree boles or intermittent flame contact from surface fuels. However, a few small regions of significant canopy consumption, associated with passive crown fire, were also observed. Mean spread rates were in the range of 0.10–0.20 m s^{-1} for EX1, and were between 0.01–0.19 m s^{-1} for EX2 (Fig. 3). A dramatic change in fire behavior in EX2 is apparent in the drop of spread rate after roughly 15 min, and again with an acceleration after 60 min. Analysis of the aerial visual imagery indicated fire front depths between 2–9 m and 1–10 m for EX1 and EX2, respectively.

3.2. Surface fuels

The pre-fire litter depth *(n=36)* for EX1 was 6 ± 3 cm and shrub layer height *(n=160)* was 82 ± 27 cm. For EX2, pre-fire litter depth *(n=55)* was 5 ± 2 cm and the shrub layer height *(n=120)* was 79 ± 19 cm. The average initial fuel loading across all plots was 1.37 kg m^{-2} and 1.68 kg m^{-2} for EX1 and EX2, respectively (Table 3). The total average consumption of these fuels was 0.92 kg m^{-2} and 1.21 kg m^{-2}. Fig. 4 shows the relationship between surface loading and consumption for each of the different sample plots. The result shows that the two variables were significantly correlated (r^2=0.87) for the particular fire conditions.

The most significant contribution, both in terms of loading and mass consumed was the needle litter. 1-hr shrub fuels also had a high percentage of consumption compared to those on the forest floor. A preliminary study of woody fuel consumption in more highly resolved size categories (*d*=0–2 mm, 2–4 mm, and 4–6.35 mm) was also conducted in association with these experiments [28]. It was found

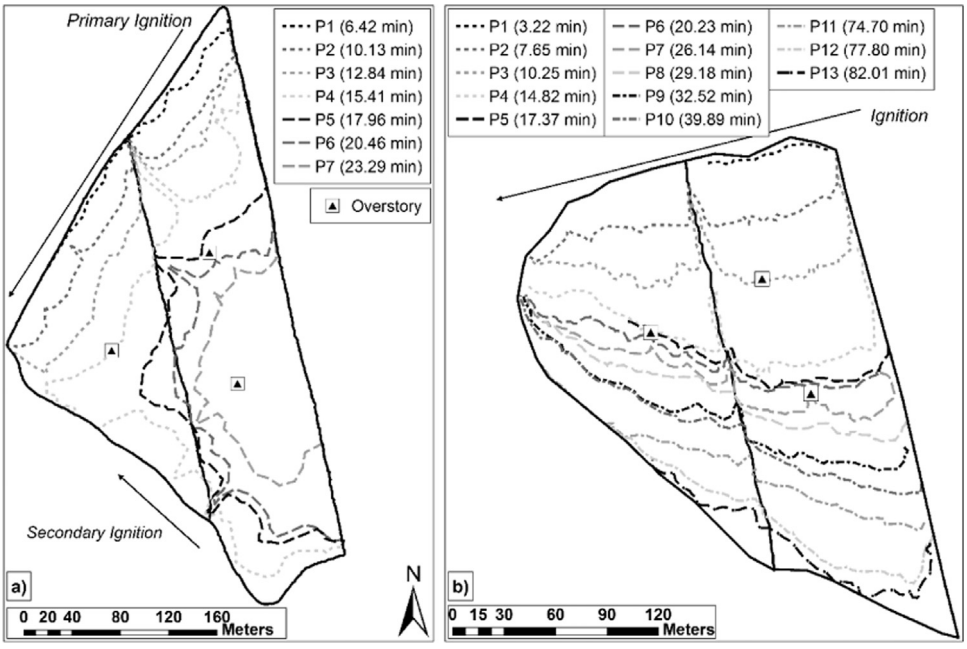

Fig. 2. IR fire isochrones from (a) EX1 and (b) EX2. Time is from ignition. Due to the secondary ignition in EX1, only the portion of the isochrones north of the South tower are considered for this experiment.

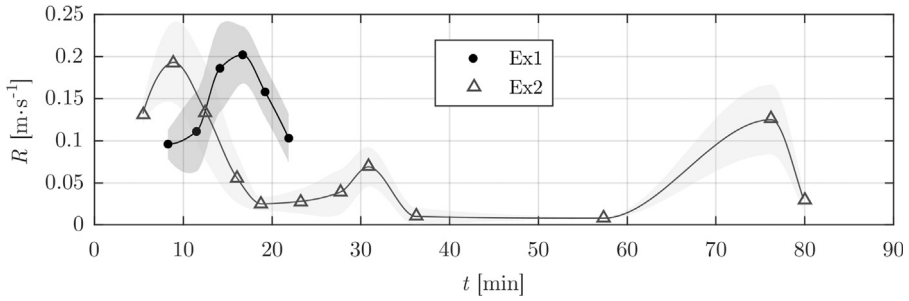

Fig. 3. Estimated mean spread rate of the fireline, measured from fire isochrones. Shaded areas represent standard deviations.

Table 3
Surface fuel measurements. Mean (standard deviation) initial surface fuel loading m_i, consumption Δm, and percent consumption $\%\Delta m$.

Fuel type	m_i (kg m^{-2})		Δm (kg m^{-2})		$\%\Delta m$	
	EX1 (*n=24*)	EX2 (*n=36*)	EX1	EX2	EX1	EX2
Needle litter	0.76 (0.12)	1.03 (0.34)	0.52 (0.15)	0.76 (0.37)	68	74
Forest floor wood	0.28 (0.16)	0.20 (0.17)	0.16 (0.16)	0.11 (0.17)	57	55
Shrub wood	0.33 (0.16)	0.45 (0.18)	0.24 (0.17)	0.34 (0.20)	73	76
Total	1.37 (0.26)	1.68 (0.42)	0.92 (0.28)	1.21 (0.45)	67	72

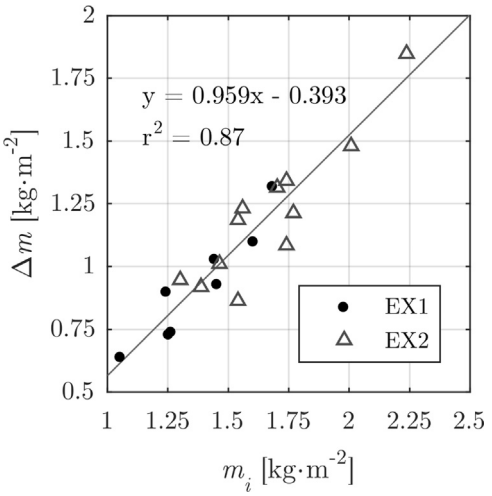

Fig. 4. Mean fuel loading and consumption at each plot. The summation of all surface fuel types in Table 3 was used for this analysis.

that only particles < 2 mm were fully consumed. However, further investigation showed that this depends on local fire intensity, with very intense fires consuming all 1-hr fuel. This can imply a requirement for more detailed size measurements when studying the behavior, such as with physics-based models.

3.3. Canopy fuels

The average characteristics of the canopy fuels, as obtained from the 10 m×10 m×1 m LiDAR CBD data, are given in Table 4. Canopy height was identified by the minimum height which contained at least 99% of the mass for a given (x,y) location. This gives an average of 14 m and 12 m for EX1 and EX2, respectively. For loadings, the mean values are 1.12 kg m^{-2} and 0.98 kg m^{-2}, with maximums of 1.78 kg m^{-2} and 1.52 kg m^{-2}. Spatial maps of canopy consumption are given in Fig. 5. The mean value for consumption is 0.19 kg m^{-2} for both experiments, with maximums of 1.00 kg m^{-2} and 1.03 kg·m^{-2}. The majority of values (86% in EX1 and 89% in EX2) are below 0.5 kg m^{-2}. The regions of negative consumption in EX1 correspond to the bands of data error, as discussed in the Methods section. However, these are mostly avoided in the region of interest, and the impact of the fire can be clearly identified in both instances.

Vertical profiles of CBD were compared between the regions of surface fire behavior and those with crown fire. The distinction was made by identifying the (x,y) locations where the consumption values are below the 90th percentile for surface fire, and above the 90th percentile for crown fire (outlined in Fig. 5). These cutoff values correspond to 0.55 kg m^{-2} and 0.51 kg m^{-2}, respectively. The occurrence of two distinct behaviors is supported by the fact that the majority of consumption is well below the cutoff, as mentioned previously, while the maximum values are approximately two times greater. Further, the crowning locations identified using this procedure (Fig. 5) agreed with post-fire visual inspection of the canopy.

In EX1, the initial canopy structure corresponding to crown fire behavior had a shorter canopy height with greater CBD at intermediate heights, up to 7 m, but peaking at 4–6 m, compared to peak CBD around 7–9 m for the remainder of the canopy (Fig. 6a,b). In EX2, the two pre-fire profiles have similar heights and shapes, and the difference appears only to be the presence of greater CBD values from 5 to 11 m in the crown fire profile compared to the surface profile (Fig. 6c,d). Peak mean CBD for the crown fire regions in both experiments is ~0.16 kg m^{-3}. In both cases, the effect of crown fire can clearly be seen in the notable reduction in CBD in the post-fire profiles (Fig. 6a,c), as compared to the majority of the canopy where the pre- and post-fire values remain quite similar (Fig. 6b,d). The crown fire behavior also led to a greater homogenization of the post-fire canopy, with a notable reduction in the variation of CBD in the lower part of the canopy. The surface fire profiles do show some consumption (comparing pre- to post-). However, this is greatest below 3–4 m, and not at all above 8–10 m, and the differences are minimal compared to the crown fire profiles. Differences in canopy height, loading, and consumption for the two cases are given in Table 4. Overall, crown fire regions show a tendency for greater loading, but the percent consumption is also significantly higher for these regions.

An interesting qualitative perspective of the canopy consumption is

Table 4
Canopy fuel structure and consumption. Mean (standard deviation) height h, initial loading m_i, consumption Δm, and percent consumption $\%\Delta m$. Fire type determined as in the text.

Fire type	h (m)		m_i (kg m^{-2})		Δm (kg m^{-2})		$\%\Delta m$	
	EX1	EX2	EX1	EX2	EX1	EX2	EX1	EX2
Surface	15	12	1.09 (0.27)	0.96 (0.20)	0.13 (0.21)	0.14 (0.13)	12	15
Crown	13	12	1.37 (0.16)	1.18 (0.16)	0.69 (0.11)	0.70 (0.14)	50	59
Average	14	12	1.12 (0.27)	0.98 (0.20)	0.19 (0.26)	0.19 (0.21)	17	19

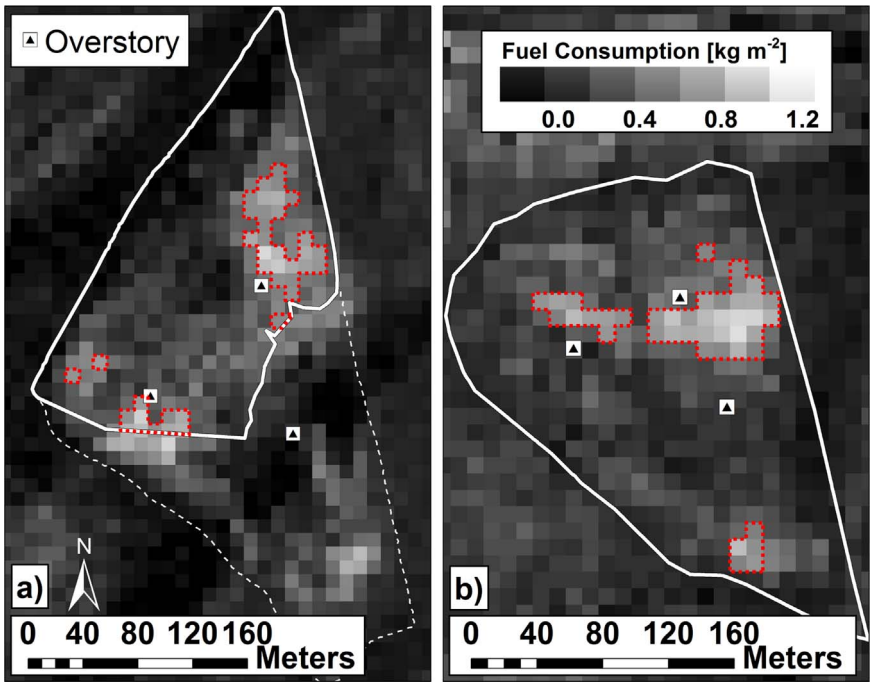

Fig. 5. Map of fuels consumption for (a) EX1 and (b) EX2. Solid lines mark the regions of interest (headfire spread). Dotted lines indicate regions of crown fire (determined following the text).

shown in Fig. 7. These pre- and post-burn images correspond to the in region of significant canopy consumption to the south of the North tower (Fig. 5), where approximately all of the live needles were consumed throughout the canopy. The percentage of 1-hr fuel consumed is more difficult to ascertain, but compared to Table 4, it appears that consumption is under-predicted in these high intensity regions. The vegetation models applied to the LiDAR have not been extensively calibrated to high intensity fires, and continued refinement may be necessary. Figure Fig. 7 also shows total consumption of shrub fuel in this region, with only very short sections of stems remaining.

3.4. Energy release

The sample size of surface fuel measurements (Table 3) did not allow for a determination of highly localized fuel consumption, so total average values were used to calculate surface fireline intensity, I_{surf}. The mean intensity values for EX1 range between 1650–3480 kW m^{-1}, while for EX2 the range is 180–4370 kW m^{-1} (Fig. 8). However, considering the effects of the variability of spread rate and fuel consumption, EX1 is estimated to have had peak surface fire intensities in excess of 4600 kW m^{-1}, while EX2 exceeded 6100 kW m^{-1} (shaded area in Fig. 8).

The above calculation does not consider canopy fuel consumption. However, as mentioned previously, visual observation suggested that most of the canopy consumption occurred as a result torching, and the mean values were only ~20% of the surface consumption (Table 3). As a result, including the energy from these fuels should result in only a minimal effect on fire behavior.

On the other hand, these estimates likely do not capture the true peaks of fire intensity observed in isolated areas where significant continuous crown fuel consumption occurred (outlined in Fig. 5). For one, the low time resolution of the spread rate calculation means that it yields average values which can obscure the more dynamic behavior. In EX2, for example, if additional information is included from a fire measurement site located in the region shown in Fig. 7, a local spread rate of ~0.4 m s^{-1} is obtained [29]. This is twice the maximum average spread rate obtained from the isochrones. Further, this canopy fuel consumption would serve to increase the energy release by a more

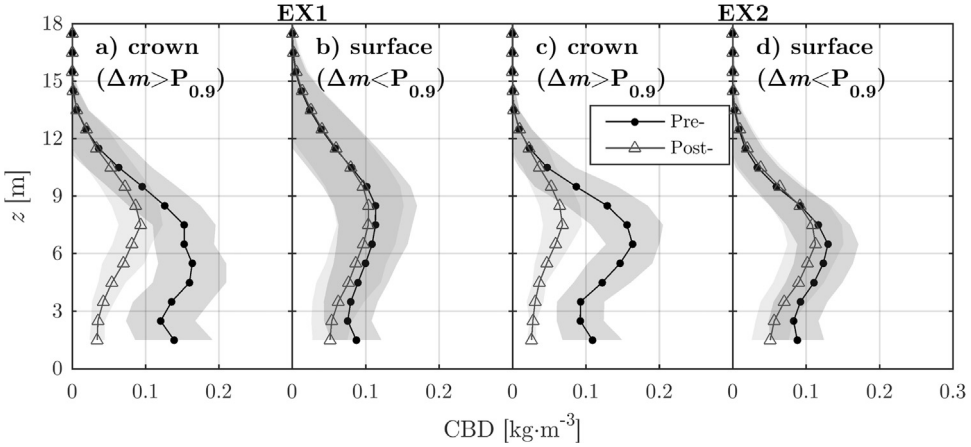

Fig. 6. Pre- (circles) and post-fire (triangles) mean profiles of CBD for (a,b) EX1 and (c,d) EX2. Profiles averaged over (a,c) areas of crown fire and (b,d) surface fire. Shaded areas are ± 1 standard deviation. The lowest bin (0–1 m) has been removed, as described in the Methods section.

Fig. 7. Pre- and post-fire fuel in region of crown fire (south of the North tower). Photos are not from identical locations, but are opposing perspectives of the same region.

significant factor. Considering total consumption of all small diameter surface and canopy fuel in this region (e.g. Fig. 7), mass consumption becomes 2.86 kg m^{-2}. Given these values, an approximate value of crown fire intensity of 21 MW m^{-1} was calculated, which is more typical of the expected values for crown fire behavior [30].

3.5. Ambient wind

Ambient wind magnitudes and directions, measured from the Control towers at a height of 12.5 m, are shown in Table 5. Values are reported for measurement periods between each fire isochrone, as wind changes may be correlated with changing features of fire behavior [9]. Both experiments were carried out under relatively light ambient overstory winds. The magnitudes were consistently lower in EX1, with a mean horizontal magnitude of 1.8 m s^{-1} during the period of interest, compared with 3.9 m s^{-1} for EX2. The peak measured values were 6.4 m s^{-1} (during P3-P4) and 11.4 m s^{-1} (during P5-P6), for the respective experiments. However, these gusts were of very short duration, as can be seen by their minimal impact on mean values during these intervals. The average ambient wind direction in EX1 was well aligned with the southeasterly direction of spread from the main ignition. In EX2 the prevailing winds had a similar direction (from the northwest), but this was oblique to the dominant spread direction by about 45°. Measurements from the other overstory towers were influenced by fire-induced winds, and are not discussed at present.

The anemometer on the north road in EX2 also gives an indication of the ambient winds below canopy height. The mean magnitude was 0.9 m s^{-1}, and represents approximately 23% of the overstory value. This should be more representative of the ambient magnitude at flame height. The mean direction was similar to that of the Control tower but tends to a more northerly direction, particularly in the early stages of the fire. This is likely a result of entrainment when the fire is initially close to the road.

Table 5
Mean (standard deviation) horizontal wind magnitude and direction (degrees from north) measured at the Control towers (12.5 m) in both experiments.

Interval	Magnitude (m s^{-1})		Direction (°)	
	EX1	EX2	EX1	EX2
Ignition-P1	1.8 (0.8)	4.6 (2.0)	305 (23)	301 (23)
P1-P2	1.0 (0.7)	3.3 (1.6)	298 (63)	295 (27)
P2-P3	2.4 (1.0)	3.7 (1.7)	5 (24)	309 (30)
P3-P4	2.7 (0.9)	3.7 (1.8)	305 (15)	312 (28)
P4-P5	1.9 (0.8)	4.1 (1.9)	290 (26)	293 (23)
P5-P6	2.1 (0.8)	4.2 (2.1)	294 (22)	295 (25)
P6-P7	1.4 (0.7)	4.3 (1.7)	354 (49)	308 (20)
P7-P8	–	4.6 (1.8)	–	313 (19)
P8-P9	–	4.7 (1.8)	–	315 (19)
P9-P10	–	3.4 (1.7)	–	314 (26)
P10-P11	–	4.1 (1.7)	–	290 (26)
P11-P12	–	3.4 (1.1)	–	325 (22)
P12-P13	–	2.1 (1.3)	–	294 (53)
Full duration	1.8 (0.9)	3.9 (1.8)	314 (43)	300 (29)

4. Discussion

4.1. Fire characteristics

Overall, the fire behavior of the two experiments was comparable, spreading as surface fires with localized regions of passive crown fire. The peak spread rate estimates were similar, though EX2 had a significant period of slow, low intensity spread through the middle of the block, with spread rates varying by an order of magnitude between the minimum and maximum. Consistency between the two experiments can be attributed to the similar fuel loadings, relatively low wind speeds, and cool temperatures. Surface fuel loadings were similar, though slightly higher values in EX2 lead to increased consumption (1.3 times EX1) and, therefore, a greater peak intensity. Both canopy fuel loadings and consumptions were also within similar ranges for the two burns. The characterization of fuels agrees with those of Clark et al. [21] for surface fuels and of Clark et al. [23] for canopy fuels in other

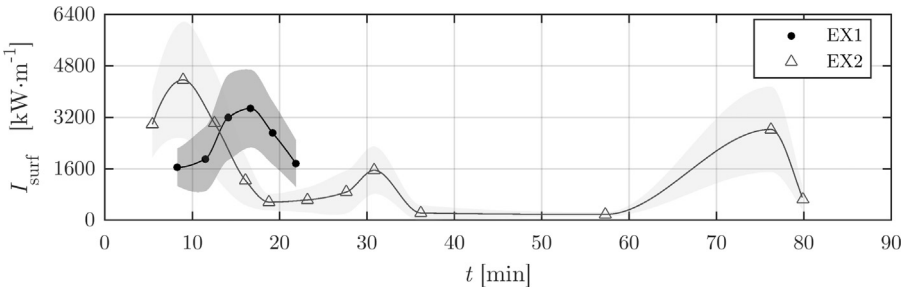

Fig. 8. Mean surface fireline intensity, I_{surf}. Shaded areas represent calculated standard deviations.

Pinelands forests. However, this study extends the work to include complementary fuels and fire intensity data necessary for the continued development of physics-based models.

Characteristics of the surface fire are comparable to other studies in forested environments with a live shrub layer. Fernandes et al. [12] reported similar ranges of spread (0.004–0.23 m s^{-1}) and fireline intensity (30–3530 kW m^{-1}) for a series of 90 head fires. These were carried out under similarly mild burning conditions. Fernandes et. al [12] developed an empirical correlation between fire intensity and flame length, of the same form as Byram [25]. Applied to EX1 and EX2, this gives flame lengths in the range of 0.8–4.7 m, and similar results are obtained for other correlations developed in forested environments [31]. This extent of surface fire flames links to the tendency for consumption in the lower canopy (up to 4 m), even in the absence of crown fire (Fig. 6).

The calculated fireline intensity was found to significantly increase when canopy fuel consumption was included for relevant regions of spread. The estimated upper bound for crown fire intensity (21,000 kW m^{-1}) is below reported extreme values for fully active crown fires in other fuel types (exceeding 90,000 kW m^{-1}) [11]. However, this is closer to values for passive and developing active crown fires reported by Van Wagner [30].

4.2. Wind and fuel

Changes in the observed fire behavior, such as the large drop in spread in EX2, are apparently not directly linked to changes in ambient wind direction or magnitude (Table 5), unlike prior studies [9]. Further, spread direction also appears to be linked more to the orientation of the ignition line than wind direction. These facts may be better understood by examining the non-dimensional Byram convective number, *Nc* [32]:

$$N_c = \frac{2gI}{\rho c_p T_o (u_o - R)^3}. \quad (2)$$

This gives the ratio of the power of the fire (related to buoyancy) to the power of the wind (related to inertia), and helps identify wind-driven ($N_c << 1$) and plume-dominated ($N_c >> 1$) fire behavior. The average ambient winds at surface level are typically low (≤5 m s^{-1} at canopy height and ≤1 m s^{-1} when accounting for the reduction below canopy height). This results in N_c on the order of 1 for periods of low to moderate intensity, and $N_c >> 1$ during crown fire activity. This indicates that the fires were not strongly wind-driven, and in fact were more sensitive to buoyancy-induced momentum. This is corroborated by observations of downwind indrafts and upright flames, particularly in the high intensity regions [29]. The dominance of the plume may explain the fact that spread direction was governed by the ignition orientation. Finally, it has been suggested that plume-dominated fires can be linked to erratic fire behavior, due to the fact that non-linear processes (radiation) may dominate [3], which can contribute to the wide range of behavior observed over relatively steady ambient conditions.

It should also be mentioned that intermittent, local gusts if ambient wind, which are not captured here, may have played a role in the observed variability in fire behavior. Sullivan and Knight [33] discussed the issues with correlating remote measurements of wind with fire behavior. This remains an issue with many experimental field campaigns, as it is very difficult to separate ambient from fire-induced winds in proximate measurements. In addition, sensor survivability is a challenge for in-situ measurement of crown fire behavior.

Pre-fire surface fuel structure can also be used to understand the fire behavior. First, the amount of surface fuel consumed was well correlated with the initial loading (Fig. 4), which is consistent with previous studies of prescribed fires in this region [21,34]. This is important given that the consumption of surface fuels largely drives the fire behavior. For example, consider the regions of high spread rate with limited canopy fuel involvement (e.g. P3-P4 in the center of the EX1 fireline, P2-P3 in EX2, when compared to Fig. 5). Given the lack of correlation with the ambient wind, this rapid spread is most likely driven by surface fuel consumption. Second, the pre-fire structure can also limit spread. The sudden and prolonged reduction in the spread of EX2 did not corresponding with a reduction in ambient wind, and appears to be associated with increased surface fuel heterogeneity. While the mean shrub loading (diameter < 6.35 mm) for the plots with low spread (*n=18*) was 0.41 kg m^{-2}, which is close to the overall mean (Table 3), the relative standard deviation was 54%. This is supported by visual observation of patchy shrub fuels in the southern portion of the block. Comparatively, a mean loading of 0.48 kg m^{-2} and a relative standard deviation 25% were found for the plots with more rapid spread, indicating an effect of fuel heterogeneity. The impact of fuel heterogeneity on fire spread has been studied previously, with critical thresholds for non-propagation suggested [35,36]. However, in the present experiments, the needle litter remains more homogeneous throughout, providing a means for continued propagation, albeit more slowly, in the absence of direct shrub-to-shrub flame spread. In general, a better quantification of both turbulence associated with fire-atmosphere interactions and fine scale fuel structure will contribute to the description of unsteady fire behavior.

The surface fuels also provide the energy necessary to support a fire in the canopy. Van Wagner [30] introduced a framework for assessing crown fire potential, which has been used extensively [37], and can serve as a baseline for understanding the transition to crown fire observed in these experiments. A critical intensity to initiate the vertical spread into canopy fuels, I_c, is calculated, based on crown base height and ignition energy [30]. In our experiments, there is no clear crown base height, with canopy fuels extending to the shrub layer (Fig. 1, Fig. 6). Taking the height of the interface of the canopy with the top of the shrub layer (~1 m) I_c=200 kW m^{-1}. This provides confirmation that ignition of these fuels can occur easily (observed as low-height canopy consumption and torching).

However, the high level of consumption and associated spread through the canopy, occurring only in certain regions (Fig. 5), is also linked to the pre-fire canopy structure (Table 4, Fig. 6). Following the theory of Van Wagner [30], a certain minimum CBD is required for fire spread in the canopy, given a particular surface spread rate. This agrees with the higher CBD present in regions of crown fire. While more studies are required to identify an exact threshold, these pre-fire profiles had peak CBD values around 0.16 kg m^{-3}. As these dense areas of crown fuel are elevated, if we consider a height of 4–5 m (roughly the bottom of the elevated band of peak CBD (Fig. 6)) the critical intensity becomes I_c=1600–2200 kW m^{-1}. This condition is still met for periods of fire spread where crown fire was observed. Likewise, Agee [38] observed a threshold for crown fire activity for a total crown bulk density of ~0.1 kg m^{-3}. While the crown bulk density was not measured here, a rough estimate can be developed from dividing the canopy fuel load by the canopy height in areas of crown fire (Table 4). Values of 0.11 kg m^{-3} and 0.10 kg m^{-3} are obtained for the two experiments, which is quite comparable. This helps to explain the transitional/passive crown fire behavior, as higher densities would be needed to support an active crown fire. The theory of Van Wagner also reinforces the fact that the presence of canopy density conducive to crowning is a necessary but not sufficient condition in the case of passive crown fire. Thus a modification to surface fire behavior, such as through increased shrub heterogeneity, can cause an interruption in the occurrence of a crown fire.

5. Conclusions

This general overview of the fire behavior observed in two experiments offers insight into the behavior and impact that fires in the PNR can have during the late winter and early spring, placing a particular

focus on remote sensing techniques. With similar pre-fire fuel loadings, the fires spread primarily through the surface fuels with moderate, but variable spread rates (0.01–0.2 m s^{-1}) and surface fireline intensities (200–4400 kW m^{-1}), though occasional torching and isolated regions of more continuous crown consumption were observed. The impacts of fuel and wind variables were considered. It was found that surface fuel consumption was well linked to initial loading, across all sample locations. Further, through the analysis of LiDAR-derived CBD profiles, a threshold of 0.16 kg·m^{-3} for the peak value is suggested to support crown fire. However, this alone is not sufficient, and the occurrence of crown fire will be strongly linked to the surface fire. Features of the wind could not be directly linked to changes in fire behavior, however, an examination of the Byram convective number showed that, for light winds, buoyancy forces should dominate at flame level. This can help account for the relatively unsteady behavior of the fires, particularly EX2. However, the role of highly local variations in surface fuels and wind gusts has not been fully captured. Focus on these aspects is recommended in future work, particularly as an improved understanding of this dynamic behavior can be of value for fire fighter safety, during both prescribed and wildland fire operations.

The number and type of measurements discussed here, both in terms of pre-fire conditions and descriptions of fire dynamics, represent a minimum necessary for the basic exploration of fire behavior. However, studies at even this level of detail are relatively uncommon for individual fires, though they are required for the initialization and testing of detailed physics-based models. While the remote sensing approaches detailed here provided a reasonable global picture, improvements can be made to the temporal scale of some measurements (IR images) and the spatial scale of others (surface fuel, wind measurements). Such improvements can shed light on the cause of the unsteady fire behavior. It is likely that the ambient wind was not a direct source, but a greater number of close proximity measurements would help answer this. The influence of the surface fuel loading and continuity could also be better characterized with more detailed spatial information. Nevertheless, this work provides a solid basis for a measurement and analysis framework for future experiments. While such studies require significant resources, they are necessary for model improvement, which will in turn help lead to a better fundamental understanding of fire behavior.

Acknowledgements

The authors wish to thank the Joint Fire Science Program (JFSP) for funding this research effort (project #12-1-03–11), and the NJFFS, particularly Division Firewarden (ret.) James Dusha and Section Firewarden Ashley House, for their strong support in the planning and execution of the experimental fires. Dr. Filkov was supported by The Tomsk State University Academic D.I. Mendeleev Fund Program.

References

[1] M.A. Finney, J.D. Cohen, S.S. McAllister, W.M. Jolly, On the need for a theory of wildland fire spread, Int. J. Wildland Fire 22 (2013) 25–36. http://dx.doi.org/10.1071/WF11117.

[2] W.M. Pitts, Wind effects on fires, Progress. Energy Combust. Sci. 17 (1991) 83–134. http://dx.doi.org/10.1016/0360-1285(91)90017-H.

[3] D. Morvan, Physical phenomena and length scales governing the behaviour of wildfires: a case for physical modelling, Fire Technol. 47 (2011) 437–460. http://dx.doi.org/10.1007/s10694-010-0160-2.

[4] N. Cheney, J. Gould, W. Catchpole, The influence of fuel, weather and fire shape variables on fire-spread in grasslands, Int. J. Wildland Fire 3 (1993) 31–44. http://dx.doi.org/10.1071/WF9930031.

[5] N. Cheney, J. Gould, Fire growth in grassland fuels, Int. J. Wildland Fire 5 (1995) 237–247. http://dx.doi.org/10.1071/WF9950237.

[6] C.B. Clements, B. Davis, D. Seto, J. Contezac, A. Kochanski, J.-.B. Fillipi, N. Lareau, B. Barboni, B. Butler, S. Krueger, Overview of the 2013 FireFlux II grass fire field experiment, Proceedings of the VII International Conference on Forest Fire Research, 2014, pp. 392-400..

[7] R.D. Ottmar, J.K. Hiers, B.W. Butler, C.B. Clements, M.B. Dickinson, A.T. Hudak, J.J. O'Brien, B.E. Potter, E.M. Rowell, T.M. Strand, Measurements, datasets and preliminary results from the RxCADRE project–2008, 2011 and 2012, Int. J. Wildland Fire 25 (2015) 1–9.

[8] D.X. Viegas, M.G. Cruz, L.M. Ribeiro, A.J. Silva, A. Ollero, B. Arrue, R. Dios, F. Gómez-Rodríguez, L. Merino, A.I. Miranda, P. Santos, Gestosa fire spread experiments Proceedings of IV International Conference on Forest Fire Research 2002 Wildland Fire Safety Summit, 2002, pp. 1–13, 2002.

[9] P.A. Santoni, A. Simeoni, J.L. Rossi, F. Bosseur, F. Morandini, X. Silvani, J.H. Balbi, D. Cancellieri, L. Rossi, Instrumentation of wildland fire: characterisation of a fire spreading through a Mediterranean shrub, Fire Saf. J. 41 (2006) 171–184. http://dx.doi.org/10.1016/j.firesaf.2005.11.010.

[10] F. Morandini, X. Silvani, Experimental investigation of the physical mechanisms governing the spread of wildfires, Int. J. Wildland Fire 19 (2010) 570–582. http://dx.doi.org/10.1071/WF08113.

[11] B.J. Stocks, M.E. Alexander, B.M. Wotton, C.N. Stefner, M.D. Flannigan, S.W. Taylor, N. Lavoie, J.A. Mason, G.R. Hartley, M.E. Maffey, Crown fire behaviour in a northern jack pine black spruce forest, Can. J. For. Res. 34 (2004) 1548–1560. http://dx.doi.org/10.1139/x04-054.

[12] P.M. Fernandes, H.S. Botelho, F.C. Rego, C. Loureiro, Empirical modelling of surface fire behaviour in maritime pine stands, Int. J. Wildland Fire 18 (2009) 698–710. http://dx.doi.org/10.1071/WF08023.

[13] B.M. Wotton, J.S. Gould, W.L. McCaw, N.P. Cheney, S.W. Taylor, Flame temperature and residence time of fires in dry eucalypt forest, Int. J. Wildland Fire 21 (2012) 270–281. http://dx.doi.org/10.1071/WF10127.

[14] E.V. Mueller, W.E. Mell, N.S. Skowronski, K.L. Clark, M.R. Gallagher, R. Hadden, A. Simeoni, Field-Scale Testing of Detailed Physics-Based Fire Behavior Models, in: Proccedings of the 5th International Fire Behavior and Fuels Conference, International Association of Wildland Fire, pp. 62–67, 2016.

[15] K.L. Clark, N. Skowronski, H. Renninger, R. Scheller, Climate change and fire management in the mid-Atlantic region, For. Ecol. Manag. 327 (2014) 306–315.

[16] J. Tedrow, Soils of New Jersey, Krieger Publishing Co, Malabar, 1986.

[17] B.R. Collins, K.H. Anderson, Plant communities of New Jersey: a study in landscape diversity, Rutgers University Press, New Brunswick, 1994.

[18] N.S. Skowronski, K. Clark, R. Nelson, J. Hom, M. Patterson, Remotely sensed measurements of forest structure and fuel loads in the Pinelands of New Jersey, Remote Sens. Environ. 108 (2007) 123–129. http://dx.doi.org/10.1016/j.rse.2006.09.032.

[19] K.L. Clark, N.S. Skowronski, M. Gallagher, H. Renninger, K. Schäfer, Effects of invasive insects and fire on forest energy exchange and evapotranspiration in the New Jersey pinelands, Agric. For. Meteorol. 166 (2012) 50–61. http://dx.doi.org/10.1016/j.agrformet.2012.07.007.

[20] D. McKeown, J. Faulring, R. Krzaczek, S. Cavilia, J. van Aardt, Demonstration of delivery of ortho imagery in realtime for local emergency response, SPIE Conference on Algorithms and Technologies for Multispectral, Hyperspectral, and Ultraspectral Imagery XVII, International Society for Optics and Photonics, 2011, 11 p., http://doi.dx.org/10.1117/12.884054.

[21] K.L. Clark, N.S. Skowronski, M. Gallagher, Fire management and carbon sequestration in pine barren forests, J. Sustain. For. 34 (2015) 125–146. http://dx.doi.org/10.1080/10549811.2014.973607.

[22] N.P. Cheney, Fire behaviourFire and the Australian Biota, Australian Academy of Science, Canberra, 1981, pp. 151–175.

[23] K.L. Clark, N.S. Skowronski, M. Gallagher, N. Carlo, M. Farrell, M.R. Maghirang, Assessment of Canopy Fuel Loading Across a Heterogeneous Landscape using LiDAR (Final Report 10-1-02-14), Joint Fire Science Program, 2013, p. 47.

[24] N.S. Skowronski, K.L. Clark, M. Duveneck, J. Hom, Three-dimensional canopy fuel loading predicted using upward and downward sensing LiDAR systems, Remote Sens. Environ. 115 (2011) 703–714. http://dx.doi.org/10.1016/j.rse.2010.10.012.

[25] G.M. Byram, Combustion of forest fuelsForest Fire: Control and Use, McGraw-Hill, New York, 1959, pp. 61–89.

[26] M.E. Alexander, Calculating and interpreting forest fire intensities, Can. J. Bot. 60 (1982) 349–357. http://dx.doi.org/10.1139/b82-267.

[27] C.E. Van Wagner, Heat of combustion, heat yield, and fire behaviour (Information Report PS-X-35), Canadian Forestry Service, 1972, p. 9.

[28] M. El Houssami, E. Mueller, A. Filkov, J.C. Thomas, N. Skowronski, M.R. Gallagher, K. Clark, R. Kremens, A. Simeoni, Experimental procedures characterising firebrand generation in Wildland fires, Fire Technol. 52 (2015) 731–751. http://dx.doi.org/10.1007/s10694-015-0492-z.

[29] E.V. Mueller, Examination of the underlying physics in a detailed wildland fire behavior model through field-scale experimentation(PhD Thesis), University of Edinburgh, 2016.

[30] C.E. Van Wagner, Conditions for the start and spread of crown fire, Can. J. For. Res. 7 (1977) 23–34. http://dx.doi.org/10.1139/x77-004.

[31] M.E. Alexander, M.G. Cruz, Interdependencies between flame length and fireline intensity in predicting crown fire initiation and crown scorch height, Int. J. Wildland Fire 21 (2012) 95–113. http://dx.doi.org/10.1071/WF11001.

[32] R.M. Nelson, Byram derivation of the energy criterion for forest and wildland fires, Int. J. Wildland Fire 3 (1993) 131–138. http://dx.doi.org/10.1071/wf9930131.

[33] A.L. Sullivan, I.K. Knight, Estimating error in wind speed measurements for experimental fires, Can. J. For. Res. 31 (2001) 401–409. http://dx.doi.org/10.1139/cjfr-31-3-401.

[34] K.L. Clark, N.S. Skowronski, M. Gallagher, W. Heilman, J. Hom, Fuel consumption and particulate emissions during fires in the New Jersey Pinelands, in: Proceedings of the 3rd Fire Behavior and Fuels Conference, International Association of Wildland Fire, p. 19, 2010.

[35] J. Nahmias, H. Téphany, J. Duarte, S. Letaconnoux, Fire spreading experiments on heterogeneous fuel beds, Appl. percolation Theory, Can. J. For. Res. 30 (2000) 1318–1328. http://dx.doi.org/10.1139/cjfr-30-8-1318.

[36] A. Simeoni, P. Salinesi, F. Morandini, Physical modelling of forest fire spreading through heterogeneous fuel beds, Int. J. Wildland Fire 20 (2011) 625–632. http://dx.doi.org/10.1071/WF09006.
[37] M.G. Cruz, M.E. Alexander, Assessing crown fire potential in coniferous forests of western North America: a critique of current approaches and recent simulation studies, Int. J. Wildland Fire 19 (2010) 377–398. http://dx.doi.org/10.1071/WF08132.
[38] J.K. Agee, The influence of forest structure on fire behavior, in: Proceedings of the 17th Annual Forest Vegetation Management Conference, 1996pp. 16–18.